DR. JULIA ARCIERO (Orcid ID : 0000-0002-2882-3653)

Article type : Original Research

Assessing the hemodynamic contribution of capillaries, arterioles and collateral arteries to vascular adaptations in arterial insufficiency

Julia Arciero[1*], Lauren Lembcke[2], Elizabeth Franko[3], Joseph Unthank[4]

[1]*Department of Mathematical Sciences, IUPUI, Indianapolis, IN 46202*

[2]*Department of Mathematics, Clemson University, Clemson, SC 29634*

[3]*Department of Mathematics, University of Scranton, Scranton, PA 18510*

[4]*Department of Surgery, Indiana University School of Medicine, Indianapolis, IN 46202*

Running Title: Vascular adaptations following occlusion

Support: NSF DMS-1559745, NSF DMS 1654019, NIH HL 42898

[*]**Corresponding Author:** Julia Arciero, jarciero@iupui.edu, 402 N. Blackford St., LD 270D, Indianapolis, IN 46202

This is the author's manuscript of the article published in final edited form as:

Arciero, J., Lembcke, L., Franko, E., & Unthank, J. (2019). Assessing the hemodynamic contribution of capillaries, arterioles and collateral arteries to vascular adaptations in arterial insufficiency. Microcirculation, 0(ja). https://doi.org/10.1111/micc.12591

Abstract

Objective. There is currently a lack of clarity regarding which vascular segments contribute most significantly to flow compensation following a major arterial occlusion. This study uses hemodynamic principles and computational modeling to demonstrate the relative contributions of capillaries, arterioles and collateral arteries at rest or exercise following an abrupt, total, and sustained femoral arterial occlusion.

Methods. The vascular network of the simulated rat hindlimb is based on robust measurements of blood flow and pressure in healthy rats from exercise and training studies. The sensitivity of calf blood flow to acute or chronic vascular adaptations in distinct vessel segments is assessed.

Results. The model demonstrates that decreasing the distal microcirculation resistance has almost no effect on flow compensation while decreasing collateral arterial resistance is necessary to restore resting calf flow following occlusion. Full restoration of non-occluded flow is predicted under resting conditions given all chronic adaptations, but only 75% of non-occluded flow is restored under exercise conditions.

Conclusion. This computational method establishes the hemodynamic significance of acute and chronic adaptations in the microvasculature and collateral arteries under rest and exercise conditions. Regardless of the metabolic level being simulated, this study consistently shows the dominating significance of collateral vessels following an occlusion.

Keywords: arterial insufficiency, arterial occlusion, model, vascular adaptation, capillaries, arterioles, collateral arteries.

List of Abbreviations

1. PAD: Peripheral Arterial Disease

2. CIA: central iliac artery
3. EIA: external iliac artery
4. FEM: femoral artery
5. IIA: internal iliac artery
6. COL: collateral
7. FEED: feed arteries
8. MID: mid-sized arterioles
9. CAP: capillaries
10. VEIN: venous system
11. THIGH: thigh region downstream of the IIA
12. PA: perforating artery
13. LA: large arteries
14. SA: small arteries/arterioles
15. C: capillaries
16. SV: small venules
17. LV: large venules
18. I: current
19. R: resistance
20. V: voltage
21. P: pressure
22. Q: flow
23. D: distal arteriolar dilation
24. C: collateral arteriolar dilation
25. E: arteriolar enlargement
26. G: growth of new arterioles or capillaries

Introduction

Peripheral arterial disease (PAD) is a pathology in which arteries within the systemic vasculature become partially or fully blocked, leading to a significant reduction in blood supply to peripheral tissues (e.g., calf and foot). Partial or gradual occlusion occurs due to progressive plaque development, whereas a sudden full occlusion occurs due to the formation of an embolism or the displacement of a plaque [1]. PAD currently affects nearly 8 million Americans and is expected to become even more prevalent with the aging of the population and increased incidence of obesity and hyperglycemia [2, 3]. Although PAD has been identified as a serious health problem for which novel therapies are greatly needed, the capability of adaptations of distinct vascular segments to improve perfusion is unknown.

Studies from war injuries have demonstrated the capability of the vasculature in young, healthy humans to compensate for an arterial occlusion [4], as has also been observed in animals. Together, these studies suggest that novel PAD therapies that can restore the

system's natural compensatory capacity would have significant efficacy. Compensatory vascular adaptations include increases in the number and/or diameters of capillaries and arterioles distal to the occlusion and increases in the numbers and/or diameters of the arteries that function as collateral pathways that bypass the occlusion [5, 6]. Numerous studies [5, 7-12] have demonstrated adaptations in these different vascular segments following an occlusion, but the relative importance of these adaptations in improving or restoring tissue perfusion is still debated [13-24].

Vascular responses to an abrupt major arterial occlusion occur on different time frames and at different locations in the vascular network. An immediate (acute) vascular response occurs within seconds to minutes of an occlusion. An example of an acute response is a sudden increase in vessel diameter due to the relaxation of vascular smooth muscle cells. A gradual (chronic) vascular response to sustained obstruction of flow occurs within days to weeks of the occlusion. An example of a chronic response is the structural remodeling of the vessel such as anatomic increases in the lumen area and wall thickness of a collateral artery (a process known as arteriogenesis) or the formation of capillaries from pre-existing capillaries (a process known as angiogenesis) [14]. In addition to the timeframe of a vascular response, the location of the response is also critical for adequate flow compensation following an occlusion. The superficial femoral artery is a typical site of occlusion in atherosclerotic disease in humans, and thus flow through collateral arteries near this site is necessary for flow compensation.

Multiple studies have shown adaptations in both collateral arteries and the distal microvasculature (arterioles and capillaries) following a major arterial occlusion on both acute and chronic time frames (summarized in Table 1). The discrepancies reported in these different studies suggest that the vascular segments most capable of improving perfusion may vary with the stage or severity of PAD. Additionally, most studies do not examine responses in all vascular segments and thus cannot make conclusions about the relative importance of each segment. An underappreciated fact is that arterial occlusion

greatly impacts the site of major resistance in the vascular tree. Figure 1 shows a typical distribution of pressures measured in a non-occluded vascular network (black data points). Under normal flow conditions, vessels in the distal microcirculation are observed as the primary site of resistance (corresponding to the site of greatest pressure drop); pressure dissipation in the larger proximal vessels is minimal [25-27]. Following a major arterial occlusion, a significant decrease in pressure occurs immediately distal to the site of occlusion [8, 19, 28-30], corresponding to a large pressure drop proximal to the microcirculation (red data points, Figure 1). This suggests that adaptations in small arteries and the microcirculation distal to the site of occlusion will have much less of an impact on flow compensation than adaptations occurring proximal to the occlusion.

Some studies have combined experimental and theoretical descriptions of the changes in resistance and/or flow following a major arterial occlusion [10, 29] to illustrate the importance of collateral arteries, but the studies did not evaluate individual effects of the numerous vascular responses to the occlusion. In an effort to quantify the effects of the multiple vascular responses on flow, this study introduces a new theoretical method based on experimental measures that can be used to evaluate the relative importance of collateral vessels and the distal arterioles and capillaries in restoring flow following an abrupt major arterial occlusion. The approach presented here is relevant to a focal occlusion of the distal femoral artery, which is one of the most common clinical problems observed in PAD. The method utilizes flow and pressure measurements from rats where robust hemodynamic data are available but is easily adaptable to other species, including man. The effects of acute and chronic adaptations of collateral arteries, arterioles, and capillaries on flow compensation are calculated. This study provides an important preliminary step in understanding and quantifying observations obtained from preclinical studies of PAD with an ultimate goal of improving the design of future experimental studies that will lead to more successful PAD therapies.

Materials and Methods

A theoretical representation (herein referred to as "the model") of the vascular network of the rat hindlimb is developed in this study (Fig 2) based on morphometric and hemodynamic measures obtained from experiments. The network geometry is defined according to anatomical descriptions of the rat hindlimb [31] (Fig 2A). Non-occluded pressures and flows [29, 32-35] are used to calculate the resistance of each vessel compartment in the model. An abrupt, total, and sustained femoral arterial occlusion is then simulated by setting D_{FEM} = 0. The pressures and flows throughout the network following the occlusion are computed using the model in the absence of any vascular adaptations. Then, experimental data from exercise and training studies [32, 36-39] are used to simulate acute and chronic vascular responses to a major arterial occlusion in the rat hindlimb, respectively. The study assumes that the immediate response to intense exercise offers a reasonable parallel to the capacity for the vasculature to respond on an acute time-frame to a sudden and total major arterial occlusion. Similarly, the gradual increase in diameter and number of vessels that results in trained animals or people is assumed to be similar to the expected capacity for structural adaptation on a chronic time-frame to an occlusion, as described in [40]. The model is also used to predict the degree of collateral dilation required to achieve experimentally observed flow values in the rat hindlimb following a major arterial occlusion under resting and maximal exercise conditions [41]. The theoretical modeling procedure is summarized in the sections below.

Vascular network geometry. Greene's description of the vascular supply to the rat hindlimb (see anatomic depiction in Figure 2A) was used to construct a simple theoretical representation of the rat hindlimb [31]. There is a direct analogy between electrical flow of current (I) through an electrical resistor (R) and the flow of blood (Q) through vessels (resistors, R); thus, the rat vasculature is described here using an electrical circuit (Figure 2B). By Ohm's law, current through a resistor is proportional to the voltage drop (ΔV) across the resistor: $I = \frac{\Delta V}{R}$. Similarly, fluid flow through a vessel is proportional to the pressure drop (ΔP) along the vessel: $Q = \frac{\Delta P}{R}$

In the model, vessel compartments are defined as resistors connected in both series and parallel according to the observed network anatomy in the rat hindlimb. In the network model, a resistor may denote a single vessel, a compartment of identical vessels connected in parallel experiencing the same metabolic and hemodynamic conditions, a series of contiguous vessels, or any combination thereof. A description of each vessel compartment is provided in Table 2.

In the theoretical vascular network (Figure 2B), flow to the hindlimb is supplied by the common iliac artery (CIA). The CIA branches into the internal iliac artery (IIA), which supplies the thigh muscles, and the external iliac artery (EIA), which supplies the calf muscles. As shown in Figure 2, the EIA flows into the femoral artery (FEM), which is the site of the occlusion. The vasculature supplying the calf muscles is defined by four compartments of parallel vessels connected in series: feed arteries (FEED, diameter >90 μm), mid-sized arteries/arterioles (MID, diameter 9-90 μm), capillaries (CAP), and veins (VEIN). Flow to the calf region depends on flow through the collateral arteries (COL) if the femoral artery is occluded. A single compartment is used to represent all of the vessels supplying blood to the thigh region downstream of the IIA (THIGH).

In this study, the collateral compartment is based on the geometry of the perforating artery (PA) in the rat hindlimb [7, 9, 22]. The rat PA extends from the internal iliac artery to the femoral/popliteal artery. During non-occluded conditions, blood flows into the perforating artery from both the femoral and internal iliac arteries [9, 31]. When the femoral artery is occluded, blood flow into the internal iliac increases and moves through the PA to the popliteal/saphenous artery to feed the calf [9]. As shown in Figure 2B, the compartment representing collateral vessels in the model extends from the distal femoral artery to the distal internal iliac artery. In reality, there are multiple collateral arteries of varying sizes connecting the femoral branch and IIA [22]. These pre-existing vessels become angiographically visible due to progressive dilation following the arterial occlusion. In the

present model, the collateral compartment is assumed to contain two large collateral arteries in parallel.

The length of the collateral arteries is defined such that pressure distal to the occlusion (before any compensations have occurred) is 14% of aortic pressure [29]. Given two parallel collateral arteries of length 2.3 × 10^4 μm and diameter 140 μm [22] and assuming a constant apparent blood viscosity of μ= 3.0 cP, the resistance of the collateral compartment is calculated to be 3.66 × 10^7 dyn·sec/cm^5 using Poiseuille's Law: $R = \frac{128L\mu}{\pi D^4}$.

Hemodynamic calculations. Under non-occluded conditions, data from multiple rat studies [29, 32, 33, 35] are used to define the flow and pressure values throughout the vascular network. Flow measurements in the hindlimb of untrained Sprague-Dawley rats obtained by Armstrong and Laughlin [33] are used to determine the calf, thigh, and total blood flow in the network. Specifically, calf flow in the model is defined as the sum of the flow through the ankle extensor and flexor. Thigh flow in the model is calculated as the sum of flow to the knee extensors, knee flexors, thigh adductors, and muscles of the rump [42, 43]. Total flow to the hindlimb is the sum of the calf flow and the thigh flow. The flow measurements in these studies were reported at both rest (pre-exercise conditions) and during exercise (maximal exercise conditions); these flow values are used to simulate non-occluded resting and exercising conditions in the model, respectively, and are listed in Table 3.

The pressures P_A, P_{distal}, P_V, P_1, P_2, P_3, P_4, and P_5 for the non-occluded case are also listed in Table 3 for resting and exercising conditions. The carotid pressure measured at rest and during maximal exercise [33] is used for the incoming pressure (P_A). The pressure at P_1 is assumed to be 96% of the carotid pressure based on reports of distal common iliac pressure [34]. Distal femoral pressure (P_{distal}) is assumed to be 10% less than the carotid pressure [29, 32]. P_2 is assumed to be equal to P_{distal}. The values of pressure in the microvasculature of the calf are calculated as fractions of femoral arterial pressure, as determined by Bohlen et al. [35]. More specifically, Bohlen et al. reported that, in the cremaster, the mean

pressure in small arteries (84.5 μm diameter), pre-capillary arterioles (9.5 μm diameter), and post-capillary venules (9.3 μm diameter) is approximately 43%, 28%, and 20% of the femoral pressure, respectively [35]. Femoral arterial pressure is calculated in this study as $P_{FEM} = (P_1+P_{distal})/2$. Assuming the same ratios of pressure in comparably-sized vessels in the calf as those reported in the cremaster, $P_3 = 0.43P_{FEM}$, $P_4 = 0.28P_{FEM}$, and $P_5 = 0.20P_{FEM}$.

Given these values of flow and pressure throughout the entire network and the collateral compartment resistance, the resistances of all remaining vessel compartments are calculated. All vessel compartment resistance values are listed in Table 2.

Under occluded conditions (i.e., an abrupt and total occlusion of the femoral artery), the value of resistance in the femoral artery and EIA is considered infinite. All of the other compartment resistances are the same as in the non-occluded case. The resulting flow and pressure values in the network are calculated according to this infinite femoral arterial resistance. Conservation of flow (analogous to Kirchoff's Law) requires that the flow entering a node must equal the flow exiting the node. For example, at node P_1, the conservation of flow guarantees that $Q_{CIA} = Q_{IIA} + Q_{EIA}$. Flow in each vessel compartment *i* is given by $Q_i = \Delta P_i/R_i$, where ΔP_i is the pressure drop along compartment *i* and R_i is the total resistance of compartment *i*. Applying flow conservation at every vessel bifurcation yields a system of linear equations that can be solved for the unknown pressures (P_{distal}, P_1, P_2, P_3, P_4, and P_5) given P_A = 120 mmHg at rest (or 127 mmHg during exercise) and P_V = 0 mmHg.

Theoretical vascular adaptations. The model is used to assess the relative contributions of the calf microvasculature and collateral arteries to vascular compensation following an abrupt femoral arterial occlusion by decreasing the vascular resistance of the collateral, feed, mid, and capillary compartments individually or in combination.

Acute Adaptations. In the model, dilation data observed during reactive hyperemia following electrical muscle stimulation [36] are used to model the maximum possible acute response of the vasculature. Boegehold and Bohlen report arteriolar dilation in the spinotrapezius immediately following contraction at 8 Hz by 62%, 60%, and 103% in vessels with resting diameter 42.3 μm, 23.2, and 10.2 [36]. The maximum factor by which the smallest arterioles dilated was about 125%.

Chronic Adaptations. Chronic adaptations are implemented in the model using experimentally observed vascular adaptations following exercise training (i.e., training corresponds to increases in capillarity, arteriolar density, and arteriole diameter) [37, 38, 44]. Laughlin et al. reported that exercise training increased white gastrocnemius muscle arteriolar density of vessels with diameter 16-20 μm by 144% [37]. Exercise training was shown to increase the capillary density (caps/mm^2) by up to 57% in the white gastrocnemius [44] and 56% in the red gastrocnemius [38]. Bohlen and Lash reported a 23% increase in diameter of 1A arterioles in spinotrapezius with exercise training [39], and Lash reported a similar 21% increase [45]. Collateral dilation data reported by Herzog et al. [22] is used to estimate maximal factors of dilation observed in primary collateral pathways (Herzog observed an increase by 114%, as reported in Table 4). The remodeling and enlargement of collateral vessels observed to occur on a chronic time frame (after 25 days) is simulated in the model according to the nearly 30% increase in collateral diameter observed by Prior et al. [9]. A summary of all acute and chronic adaptations is provided in Table 4. The experimental basis for each vascular response simulated by the model is listed as well as the factor by which the vessel compartment resistance must be multiplied to simulate each adaptation. If multiple responses are simulated together, the changes in arteriolar resistance are combined via multiplication.

Model simulations. Previously obtained experimental measures [41] of flow in the rat hindlimb are used in this study to predict the degree of collateral vessel dilation that would be necessary to achieve the flow measured in these experiments in the presence or

absence of other simulated vascular adaptations. Ziegler et al. [41] measured hindlimb perfusion in young healthy Wistar Kyoto rats under non-occluded and occluded conditions at rest and during electrically stimulated calf muscle contraction.

Model predicted flow values when simulating acute vascular responses are compared with venous flow data collected within three minutes of occlusion [41]. Model predicted flow values when simulating chronic vascular responses are compared with venous flow data collected two weeks post-ligation [41]. Femoral venous outflow values at contraction frequencies of 0 Hz and 12 Hz induced by electrical field stimulation were used to compare model simulations of resting and exercising conditions, respectively. Table 5 provides a summary of the flow ratios (defined as the ratio of experimental case flow to resting non-occluded flow) measured by Ziegler et al. [41] in the rat hindlimb under resting and maximally stimulated conditions.

Results

Acute vascular adaptations at rest. The theoretical model is used to simulate acute vascular adaptations (Table 4A) to an occlusion under resting conditions; the resulting model predictions of flow and pressure are depicted in Figure 3. If there are no vascular adaptations simulated in response to the occlusion, the ratio of occluded to non-occluded flow is 0.15 (Figure 3A, blue). If the diameters of the mid-sized arterioles and feed arteries of the calf are both increased by 123%, the occluded to non-occluded flow ratio is 0.16 (red). The model is used to predict the flow ratio of occluded to non-occluded flow as the diameter of collateral arteries is varied by a factor between 1 and 2 (Figure 3A, green). The experimentally-measured flow ratio of 0.5 is depicted as a dashed black line in Figure 3A. The intersection of this dashed line with the green curve shows that an increase in collateral diameter by 54% is needed to obtain the experimentally-observed flow ratio of 0.5. If the collateral arterial diameter is increased together with a reduction in the resistance of the distal tree arterioles/arteries, the experimentally-observed flow ratio is reached if collateral arteries dilate by 50% (black). The corresponding values of pressures (P_1 and P_{distal})

predicted throughout the theoretical network are depicted for each of these cases in Figure 3B.

Summary of acute and chronic vascular adaptations at rest. Combinations of acute and chronic vascular adaptations following a major arterial occlusion are simulated in the model according to the definitions listed in Table 4. Importantly, all chronic adaptations are simulated while simultaneously assuming a 27% enlargement in the diameter of the collateral vessel. Theoretical predictions of calf flow (i.e, flow to the compartments downstream of the occlusion, also known as the collateral-dependent region) are compared with non-occluded flow to the calf, and this flow ratio is provided in Figure 4 for multiple scenarios. The combinations chosen account for simulated cases of angiogenesis (growth of new distal arterioles and capillaries, "G"), arteriogenesis (27% enlargement in collateral diameter), and collateral dilation ("C"). A "C" label in Figure 4 indicates that a 100% increase in collateral diameter was simulated. The combinations of responses that are not depicted in Figure 4 gave similar results to those shown. The model predicts that no adaptation alone can restore flow to its non-occluded value. Combined chronic vascular adaptations with collateral arterial dilation provide the only theorized method for restoring flow to its non-occluded level (Chronic GCED case).

Acute and chronic vascular adaptations during rest and exercise conditions. Figure 5 shows the model-predicted ratios of occluded to non-occluded flow when all acute responses (DC) are present (green) and when all chronic responses (GCED) are present (yellow). Again, 100% dilation of the collateral artery is assumed for the vascular response labeled "C." These flow ratio comparisons are calculated for simulated rest conditions and simulated exercise conditions. The model predicts that the combined chronic vascular responses are sufficient to restore resting normal flow, but can only restore about 75% of exercise flow. This comparison also shows that both acute and chronic vascular adaptations are much more successful at restoring flow under rest conditions; the ability to compensate for an occlusion is significantly reduced under exercise conditions.

Model comparison with experimental values for rest and exercise conditions. When both acute and chronic vascular adaptations are simulated, the model is used to predict the degree of collateral dilation that would be necessary to yield the experimentally-observed flow ratios listed in Table 5 (Figure 6, blue bars) or to restore flow to the non-occluded rest or exercise value (Figure 6, yellow bars). Note, the blue bars in panel A for the acute case give the values of the intersection points of the green and black curves with the dashed black line in Figure 3.

The significant dependence on collateral dilation is evident from the minimal difference between factors predicted when the collateral dilates alone or in combination with distal arteriolar dilation, regardless if the response is acute or chronic. As expected, a high degree of collateral dilation is needed to restore non-occluded flow during resting conditions and to an even greater extent during exercising conditions. In Figure 6C and 6D, the number of collateral vessels is varied to show the effect of increasing the number of collateral vessels on the occluded to non-occluded flow ratio. No adaptations to the distal microcirculation are included. Model predictions are shown for collaterals vessels of diameter 100 μm (black), 140 μm (blue), or 200 μm (red). While complete compensation (fraction of control flow equal to 1) is never attained, flow is restored to 90% of its non-occluded value for about 30 collateral vessels of diameter 200 μm or 135 collateral vessels of diameter 140 μm. As expected, the ability to compensate is compromised under exercising conditions (panel D), showing only a 50% restoration of flow when there are 200 collateral vessels of diameter 100 μm, as opposed to nearly 80% under resting conditions.

Discussion

This study offers a theoretical approach to assist in understanding the contribution of adaptations in various vascular segments in PAD and the potential efficacy of PAD therapies that promote new vessel formation and/or dilation of existing vessels to restore tissue perfusion. By providing a computational explanation of the relationships among flow,

resistance, and pressure in the rat hindlimb pre- and post-occlusion, this study presents a strong case for the essential role of collateral dilation for significant compensation to occur following occlusion in this model. Importantly, the methods and resources developed in this study can be utilized in other models and species to provide critical insight for understanding the relative compensation of distinct vascular segments.

Acute and chronic vascular responses to a major arterial occlusion in the rat hindlimb are simulated based on experimental data from exercise and training studies [32, 36-39], respectively. The model shows that an occlusion shifts the site of primary vascular resistance from arterioles to collateral arteries and that maximal changes to the number and/or diameter of arterioles supplying the calf region of the rat hindlimb have very little impact on flow restoration (Figure 3B and Figure 4). The model uses hemodynamic calculations to demonstrate the reliance on diameter changes to the collateral compartment to cause any significant flow compensation following a complete occlusion. The minimal difference between the curves for no compensation (blue) and distal arteriolar dilation (red) in Figure 3A indicates that adaptations to the microcirculation alone make almost no difference following an occlusion without collateral dilation.

The current model predicts that vascular adaptations of large collateral vessels are necessary for flow restoration even to resting muscle. This prediction is consistent with the acute dilation of collaterals [9, 22], the increase in perfusion observed with collateral growth [5, 15], and the restoration of perfusion in PAD patients with bypass grafts which function as large collaterals [46]. As seen in Figure 5, the ability of vessels to compensate for a major arterial occlusion is severely reduced under exercise conditions. In particular, the model predicts that full restoration of non-occluded flow is possible under resting conditions given all chronic vascular adaptations (Table 4), but is predicted to yield at most 75% of non-occluded flow under exercise conditions. This is seen in the clinic, as well, when PAD patients experience pain with walking or when the distance they are able to walk becomes greatly reduced.

Figure 6 gives predicted values of collateral dilation that would be necessary to achieve either experimentally observed levels of flow or full compensation to a major arterial occlusion. However, the predicted values of collateral dilation are not realistic since the capacity for collaterals to enlarge is limited; thus, the model suggests that the addition of more collaterals (and perhaps even smaller collaterals) can offer flow improvements (Figure 6C-6D). The figure does not take into account, however, that the functional capacity of muscles following a major arterial occlusion may be reduced and thus require less flow than under normal exercise conditions (e.g., studies have described functional limitations in PAD to reflect diminished blood flow induced by arterial obstruction [47-50]). Therefore, the results of this figure should be interpreted as the maximum changes that would be necessary to restore flow to the collateral-dependent region at rest or during exercise.

The primary conclusion of this study regarding the importance of collateral dilation/enlargement is consistent with previous work in humans and animal models. For example, Matas [17] and Shepherd [18] described the capacity for acute vascular compensation to occlusion in man and implicated the importance of collaterals. Rosenthal et al. demonstrated the importance of acute collateral dilation following a major arterial occlusion in dogs [51]. Sanne and Sivertsson [20] showed that the majority of post-occlusion total vascular resistance resides in the collateral vessels and that after 5 weeks of the occlusion there was a significant decrease in resistance of collaterals but not of the distal microvasculature. Longland [21], Herzog et al. [22], and Lundberg et al. [23] all showed significant dilation and/or enlargement of collateral arteries. Hershey et al. [15] concluded that capillary sprouting cannot replace or functionally compensate for an occluded artery and that the growth of collateral vessels provides a much more efficient mechanism for flow compensation following a major occlusion.

Model limitations. As with any model, simplifying assumptions are made in this study to provide a basic model that gives insight into the contribution of distinct vascular segments to

restoring flow following a major arterial occlusion. However, it is important to note that vascular occlusions due to atherosclerotic disease occur in various locations throughout the vascular tree, and the capacity for the vasculature to adapt and the relative contribution of different vascular segments will depend on the location and extent of the occlusion. The current theoretical model is based upon a commonly used rat model of femoral artery ligation, but model predictions could differ for other sites of occlusion.

In addition, the model is based on hemodynamic and vascular network information from the rat, but model results may differ among species, strains and individual animals due to differences in branching patterns and the number and size of pre-existing vessels that can function as collaterals. Variance in the diameters of collateral arteries across species tends to be more significant than the diameters of resistance arterioles. For example, after femoral artery occlusion, collateral diameters have been measured to be approximately 2-4 mm in humans [24], 150 μm in rats [22], and 40 μm in mice [5]. Differences in imaging techniques (e.g., magnetic resonance angiography versus x-ray angiography) may also lead to dramatically different observations of collateral vessels [15, 19]. Techniques with greater resolution can identify increases in collateral diameter more accurately than other techniques. Thus, limitations in the imaging techniques used in different studies may explain why there is debate regarding the pre-existence or de novo development of collateral vessels [52]. The reporting of new vessels may actually correspond to the enlargement of vessels which had previously been too small to detect.

Finally, the presence of vascular risk factors associated with endothelial dysfunction may also compromise vascular compensation and change the relative vessel contributions. Factors such as obesity, hypertension, or diabetes may significantly alter model assumptions and resulting predictions [53-55].

Perspectives

Animal and clinical studies have shown limited effectiveness of vasodilatory drugs in treating PAD [56]. As the current study indicates, the dilation of blood vessels must be targeted to specific vessels (i.e., collateral arteries in certain locations) to cause any considerable effect on restoring flow for PAD patients, since general or untargeted vasodilation may cause undesirable vascular responses that will not improve the quality of life for PAD patients. Thus, this study motivates further experimental and theoretical studies that will lead to the development of targeted therapies that can restore tissue perfusion in PAD patients without relying on invasive surgery options.

Acknowledgements

This work is supported by NSF DMS-1559745, NSF DMS-1654019, and NIH HL 42898. The authors acknowledge the multiple undergraduate students who have assisted with this project, including M. Kennedy, S. Willoughby, A. Greenwood, and M. Burch.

References

1. Krishna, S.M., J.V. Moxon, and J. Golledge, *A review of the pathophysiology and potential biomarkers for peripheral artery disease.* Int J Mol Sci, 2015. **16**(5): p. 11294-322.
2. Gornik, H.L., *Rethinking the morbidity of peripheral arterial disease and the "normal" ankle-brachial index.* J Am Coll Cardiol, 2009. **53**(12): p. 1063-4.
3. Hirsch, A.T., et al., *Peripheral arterial disease detection, awareness, and treatment in primary care.* JAMA, 2001. **286**(11): p. 1317-24.
4. DeBakey, M.E. and F.A. Simeone, *Battle injuries of the arteries in World War II; an analysis of 2,471 cases.* Ann Surg, 1946. **123**: p. 534-79.
5. Chalothorn, D., et al., *Catecholamines augment collateral vessel growth and angiogenesis in hindlimb ischemia.* Am J Physiol Heart Circ Physiol, 2005. **289**(2): p. H947-59.
6. Faber, J.E., et al., *A brief etymology of the collateral circulation.* Arterioscler Thromb Vasc Biol, 2014. **34**(9): p. 1854-9.

7. Unthank, J.L., J.C. Nixon, and J.M. Lash, *Early adaptations in collateral and microvascular resistances after ligation of the rat femoral artery.* J Appl Physiol (1985), 1995. **79**(1): p. 73-82.
8. Unthank, J.L., J.C. Nixon, and M.C. Dalsing, *Acute compensation to abrupt occlusion of rat femoral artery is prevented by NO synthase inhibitors.* Am J Physiol, 1994. **267**(6 Pt 2): p. H2523-30.
9. Prior, B.M., et al., *Time course of changes in collateral blood flow and isolated vessel size and gene expression after femoral artery occlusion in rats.* Am J Physiol Heart Circ Physiol, 2004. **287**(6): p. H2434-47.
10. Yang, H.T., et al., *Prior exercise training produces NO-dependent increases in collateral blood flow after acute arterial occlusion.* Am J Physiol Heart Circ Physiol, 2002. **282**(1): p. H301-10.
11. Yang, H.T., R.W. Ogilvie, and R.L. Terjung, *Peripheral adaptations in trained aged rats with femoral artery stenosis.* Circ Res, 1994. **74**(2): p. 235-43.
12. Hogan, R.D. and L. Hirschmann, *Arteriolar proliferation in the rat cremaster muscle as a long-term autoregulatory response to reduced perfusion.* Microvasc Res, 1984. **27**(3): p. 290-6.
13. Wahlberg, E., *Angiogenesis and arteriogenesis in limb ischemia.* J Vasc Surg, 2003. **38**(1): p. 198-203.
14. Annex, B.H., *Therapeutic angiogenesis for critical limb ischaemia.* Nature Reviews. Cardiology, 2013. **10**(7): p. 387-396.
15. Hershey, J.C., et al., *Revascularization in the rabbit hindlimb: dissociation between capillary sprouting and arteriogenesis.* Cardiovasc Res, 2001. **49**(3): p. 618-25.
16. Ito, W.D., et al., *Angiogenesis but not collateral growth is associated with ischemia after femoral artery occlusion.* Am J Physiol, 1997. **273**(3 Pt 2): p. H1255-65.
17. Matas, R., *I. Testing the Efficiency of the Collateral Circulation as a Preliminary to the Occlusion of the Great Surgical Arteries.* Ann Surg, 1911. **53**(1): p. 1-43.
18. Shepherd, J.T., *The effect of acute occlusion of the femoral artery on the blood supply to the calf of the leg before and after release of sympathetic vasomotor tone.* Clin Sci, 1950. **9**(4): p. 355-65.
19. Rosenthal, S.L. and A.C. Guyton, *Hemodynamics of collateral vasodilatation following femoral artery occlusion in anesthetized dogs.* Circ Res, 1968. **23**(2): p. 239-48.
20. Sanne, H. and R. Sivertsson, *The effect of exercise on the development of collateral circulation after experimental occlusion of the femoral artery in the cat.* Acta Physiol Scand, 1968. **73**(3): p. 257-63.
21. Longland, C.J., *The collateral circulation of the limb; Arris and Gale lecture delivered at the Royal College of Surgeons of England on 4th February, 1953.* Ann R Coll Surg Engl, 1953. **13**(3): p. 161-76.

22. Herzog, S., et al., *Collateral arteries grow from preexisting anastomoses in the rat hindlimb.* Am J Physiol Heart Circ Physiol, 2002. **283**(5): p. H2012-20.
23. Lundberg, G., et al., *A rat model for severe limb ischemia at rest.* Eur Surg Res, 2003. **35**(5): p. 430-8.
24. Ziegler, M.A., et al., *Marvels, mysteries, and misconceptions of vascular compensation to peripheral artery occlusion.* Microcirculation, 2010. **17**(1): p. 3-20.
25. Green, H.D., C.E. Rapela, and M.C. Conrad, *Resistance (conductance) and capacitance phenomena in terminal vascular beds*, in *Handbook of Physiology*, W.F. Hamilton and P. Dow, Editors. 1963, American Physiological Society. p. 935.
26. Landis, E.M. and J.R. Pappenheimer, *Exchange of substances through the capillary walls*, in *Handbook of Physiology*, W.F. Hamilton and P.Dow, Editors. 1963, American Physiological Society. p. 961.
27. Landis, E.M., *Capillary pressure and capillary permeability.* Physiol Rev, 1934. **14**: p. 404-481.
28. Conrad, M.C. and H.D. Green, *Hemodynamics of Large and Small Vessels in Peripheral Vascular Disease.* Circulation, 1964. **29**: p. 847-53.
29. Unthank, J.L., J.C. Nixon, and M.C. Dalsing, *Inhibition of NO synthase prevents acute collateral artery dilation in the rat hindlimb.* J Surg Res, 1996. **61**(2): p. 463-8.
30. Smith, G.W. and D.C. Sabiston, Jr., *A study of collateral circulation in vascular beds.* Arch Surg, 1961. **83**: p. 702-6.
31. Greene, E., *Anatomy of the rat*. 1935, Philadelphia,: The American philosophical society. xi, 370 p.
32. Lash, J.M., J.C. Nixon, and J.L. Unthank, *Exercise training effects on collateral and microvascular resistances in rat model of arterial insufficiency.* Am J Physiol, 1995. **268**(1 Pt 2): p. H125-37.
33. Armstrong, R.B. and M.H. Laughlin, *Exercise blood flow patterns within and among rat muscles after training.* Am J Physiol, 1984. **246**(1 Pt 2): p. H59-68.
34. Meininger, G.A., K.L. Fehr, and M.B. Yates, *Anatomic and hemodynamic characteristics of the blood vessels feeding the cremaster skeletal muscle in the rat.* Microvasc Res, 1987. **33**(1): p. 81-97.
35. Bohlen, H.G., R.W. Gore, and P.M. Hutchins, *Comparison of microvascular pressures in normal and spontaneously hypertensive rats.* Microvasc Res, 1977. **13**(1): p. 125-30.
36. Boegehold, M.A. and H.G. Bohlen, *Arteriolar diameter and tissue oxygen tension during muscle contraction in hypertensive rats.* Hypertension, 1988. **12**(2): p. 184-91.
37. Laughlin, M.H., et al., *Exercise training produces nonuniform increases in arteriolar density of rat soleus and gastrocnemius muscle.* Microcirculation, 2006. **13**(3): p. 175-86.

38. Gute, D., et al., *Regional changes in capillary supply in skeletal muscle of high-intensity endurance-trained rats.* J Appl Physiol (1985), 1996. **81**(2): p. 619-26.
39. Lash, J.M. and H.G. Bohlen, *Functional adaptations of rat skeletal muscle arterioles to aerobic exercise training.* J Appl Physiol (1985), 1992. **72**(6): p. 2052-62.
40. Laughlin, M.H. and B. Roseguini, *Mechanisms for exercise training-induced increases in skeletal muscle blood flow capacity: differences with interval sprint training versus aerobic endurance training.* J Physiol Pharmacol, 2008. **59 Suppl 7**: p. 71-88.
41. Ziegler, M.A., et al., *Novel method to assess arterial insufficiency in rodent hind limb.* J Surg Res, 2016. **201**(1): p. 170-80.
42. Franken, R.J., et al., *Anatomy of the feeding blood vessels of the cremaster muscle in the rat.* Microsurgery, 1996. **17**(7): p. 402-8.
43. Nasir, S., et al., *New experimental composite flap model in rats: gluteus maximus-tensor fascia lata osteomuscle flap.* Microsurgery, 2003. **23**(6): p. 582-8.
44. Gute, D., M.H. Laughlin, and J.F. Amann, *Regional changes in capillary supply in skeletal muscle of interval-sprint and low-intensity, endurance-trained rats.* Microcirculation, 1994. **1**(3): p. 183-93.
45. Lash, J.M., *Contribution of arterial feed vessels to skeletal muscle functional hyperemia.* J Appl Physiol (1985), 1994. **76**(4): p. 1512-9.
46. Heberer, G., vanDongen, R.J.A.M., *Vascular Surgery*. 1989, New York: Springer.
47. Hamburg, N.M. and G.J. Balady, *Exercise rehabilitation in peripheral artery disease: functional impact and mechanisms of benefits.* Circulation, 2011. **123**(1): p. 87-97.
48. Pipinos, II, et al., *The myopathy of peripheral arterial occlusive disease: part 1. Functional and histomorphological changes and evidence for mitochondrial dysfunction.* Vasc Endovascular Surg, 2007. **41**(6): p. 481-9.
49. Schieber, M.N., et al., *Muscle strength and control characteristics are altered by peripheral artery disease.* J Vasc Surg, 2017. **66**(1): p. 178-186 e12.
50. Regensteiner, J.G., et al., *Chronic changes in skeletal muscle histology and function in peripheral arterial disease.* Circulation, 1993. **87**(2): p. 413-21.
51. Rosenthal, S.L. and A.C. Guyton, *Hemodynamics of collateral vasodilatation following femoral artery occlusion in anesthetized dogs.* Circulation Research, 1968. **23**: p. 239-248.
52. Simons, M., *Angiogenesis: where do we stand now?* Circulation, 2005. **111**(12): p. 1556-66.

53. Giugliano, G., et al., *The prognostic impact of general and abdominal obesity in peripheral arterial disease.* Int J Obes (Lond), 2010. **34**(2): p. 280-6.
54. Marso, S.P. and W.R. Hiatt, *Peripheral arterial disease in patients with diabetes.* J Am Coll Cardiol, 2006. **47**(5): p. 921-9.
55. Clement, D.L., M.L. De Buyzere, and D.A. Duprez, *Hypertension in peripheral arterial disease.* Curr Pharm Des, 2004. **10**(29): p. 3615-20.
56. Coffman, J.D., *Vasodilator drugs for peripheral vascular disease.* N Engl J Med, 1979. **301**(3): p. 159-60.
57. Lash, J.M., *Exercise training enhances adrenergic constriction and dilation in the rat spinotrapezius muscle.* J Appl Physiol (1985), 1998. **85**(1): p. 168-74.
58. Fronek, K. and B.W. Zweifach, *Microvascular pressure distribution in skeletal muscle and the effect of vasodilation.* Am J Physiol, 1975. **228**(3): p. 791-6.
59. Zweifach, B.W., et al., *Micropressure-flow relationships in a skeletal muscle of spontaneously hypertensive rats.* Hypertension, 1981. **3**(5): p. 601-14.

TABLE 1: Summary of acute and chronic vascular responses observed in experimental settings in multiple species.

Reference	Species	Model	Time Points	Primary outcome
Chalothorn [5]	Mouse	Unilateral, distal femoral artery occlusion	0-21 days	Increased **perfusion through adductor muscles**, maximal at day 7 **Plantar foot perfusion** decreased ~80% acutely post-occlusion and recovered to >40% at days 7-21 **Collateral luminal diameter** was increased 60% at 21 days The **number of α-smooth muscle positive vessels** increased 45% in the non-ischemic adductor muscles.

				The **number of capillaries** per muscle fiber in the gastrocnemius muscle increased 21% (note there was a 71% increase in capillary density but a decrease in fiber size, and possibly fiber number).
Hershey [15]	Rabbit	Femoral artery excision	5, 10, 20, 40 days	**Maximum capillary density** (~60% increase in adductor muscle) observed at 5 days temporally associated with ischemia; decreased to baseline by day 20. **Collateral growth** observed after day 5 and continued through day 40 was associated with increased perfusion, not ischemia
Herzog [22]	Rat	Femoral artery occlusion, distal to the arteria femoralis profunda	24 h, 3 d, 7 d, 21 d	Total number of angiographically visible **collateral arteries** increased from 2.3 to 5.3 after 7 days of occlusion and to 7.3 after 21 days of occlusion. The **midzone index** (ratio of midzone collateral diameter to diameter of the femoral artery) increased from 0.17 to 0.46 after 7 days of occlusion and decreased to 0.31 after 21 days of occlusion The total **length of the collateral artery** increased by 21% within 7 days after occlusion and by 39% within 21 days after occlusion
Ito [16]	Rabbit	Mid--femoral artery occlusion, bilateral	0, 1, 3 weeks	Acute reductions in **muscle blood flow** of 95% of maximum in lower adductors and lower limb. No reduction observed in proximal adductors **Maximal collateral conductance** increased six fold at 1 wk and only an additional 25% by 3 wks.

				Capillary density increased in ischemic gastrocnemius <50%. **Collateral growth** occurred in non-ischemic adductor muscles.
Longland [21]	Rabbit	Femoral artery ligation	10 minutes and 1, 2, 3 months	Increase in **collateral diameter** by 100% after 3 months
Rosenthal [51]	Dog	Femoral artery occlusion, distal to profunda femoris	2-60 minutes	**Flow** reached 58% of control after 70 seconds of occlusion and pressure reached 53% of control. Flow and pressure increased an additional 12% after one hour **Collateral conductance** increased 277% from minimum in 70 seconds and continued to increase an additional 178% in one hour **Peripheral vessels** constricted slightly after occlusion and dilated to a constant level within 1 minute
Sanne [20]	Cat	Superficial and deep femoral artery occlusion	0 days, 5 weeks	**Collateral resistance** decreased threefold 5 weeks after the occlusion Five weeks after occlusion, **collateral resistance** was 30% less in the trained group than the untrained group There was no change in **resistance of distal vascular bed** due to the occlusion or due to training
Shepherd [18]	Human	Acute femoral artery occlusion	0-10 minutes	**Initial flow** decreased to one-sixth of the resting value following occlusion **Resting flow** was restored at 2 minutes post occlusion Following exercise, **calf flow** with femoral occlusion was between 1 and 44% of calf flow

				without occlusion

Table 2. Description of vessels composing each compartment in the model. The resistance of each compartment under non-occluded conditions is calculated from the flow and pressure values provided in Table 3.

Vessel Compartment	**Compartment Description**	**Non-occluded Resistance** (dyn·sec/cm^5)
CIA	Single vessel	5.45 ×10^4
EIA + FEM	Single vessels connected in series	3.82 ×10^5

IIA	Single vessel	1.04×10^5
COL	Two large collateral arteries in parallel	3.66×10^7
THIGH	Entire microcirculation feeding the thigh muscle	1.56×10^6
FEED	Set of parallel vessels supplying the calf, D > 90 μm	3.20×10^6
MID	Set of parallel vessels supplying the calf, 9 < D < 90 μm	8.71×10^5
CAP	Set of parallel vessels, D < 9 μm	4.97×10^5
VEIN	Entire venous system draining the calf	1.17×10^6

Table 3. (Top) Vascular network pressure values (in mmHg, rounded to the nearest whole unit) under non-occluded conditions. (Bottom) Flow values under non-occluded conditions.

Pressure node	**Pressure at rest** (mmHg)	**Pressure at Maximum Exercise** (mmHg)	**Reference**
Carotid	120	127	[33]

(P_A)			
P_1	115	122	[34]
P_{distal}	108	114	[29, 32]
P_2	108	114	assumption
P_3	48	57	[35]
P_4	31	33	[35]
P_5	22	24	[35]
P_v	0	0	assumption

Region	Flow at Rest (cm^3/sec)	Flow at Maximum Exercise (cm^3/sec)	Reference
Calf	0.025	0.102	[33]
Thigh	0.092	0.265	[33]
Total	0.117	0.367	[33]

Table 4. Summary of simulated vascular responses to an abrupt and total major arterial occlusion. (A) Acute vascular responses. (B) Chronic vascular responses.

A. Acute Vascular Responses

Label	Vascular Adaptation (model)	Vascular Adaptation (experiment)	Maximum Observed Increase	Multiplicative Factor for Resistance
D	Distal arteriolar dilation	Arteriole dilation in stimulation-induced hyperemia	123% [36, 57]	$(2.23)^{-4}$

C	Collateral arterial dilation	Collateral arterial dilation	114% [22]	Varied

B. Chronic Vascular Responses

(responses are in addition to an assumed 27% enlargement in collateral diameter)

Label	Vascular Adaptation (model)	Vascular Adaptation (experiment)	Maximum Observed Increase	Multiplicative Factor for Resistance
E	Distal arteriolar enlargement	Arteriole enlargement after exercise training	23% [39]	$(1.23)^{-4}$
D	Distal arteriolar dilation	Arteriole dilation in stimulation-induced hyperemia	123% [36, 57]	$(2.23)^{-4}$
G	Growth of new distal arterioles	Arteriolar density increase after exercise training	144% [37]	$(2.44)^{-1}$
G	Growth of new capillaries	Capillary density increase after exercise training	57% [38, 44]	$(1.57)^{-1}$
C	Collateral arterial dilation	Collateral arterial dilation	114% [22]	Varied

Table 5. Experimental Flow Results

Experimental Case	Femoral Venous Outflow (measured, [41]) $\left(\frac{ml}{min}\right)$	Flow Ratio $\left(\frac{experimental\ flow}{resting\ non-occluded\ flow}\right)$
Rest Non-Occluded	2.18	1.00
Rest Acute	1.09	0.50
Rest Chronic	1.53	0.70
Max Stimulation (12Hz) Non-Occluded	10.27	4.71
Max Stimulation (12Hz) Acute	2.13	0.98
Max Stimulation (12Hz) Chronic	3.13	1.44

Figure Captions

Figure 1. Experimentally observed pressures throughout the vascular network of rats, cats, and dogs under normal conditions and after major arterial occlusion. Data points are taken from the following studies: **o**, Unthank et al. (rat femoral artery) [29]; ***,** Unthank et al. (rat femoral artery) [8]; ◊, Rosenthal and Guyton (dog femoral artery) [19]; ♦, Meininger et al. (rat, no occlusion) [34]; □, Bohlen et al. (rat, no occlusion) [35]; ✵**,+**, Fronek and Zweifach (cat, no occlusion) [58]; and Δ, Zweifach (rat, no occlusion) [59]. Black data points are collected from the non-occluded limb; red data points are collected from the occluded limb immediately following occlusion (within 30 seconds). Here, vessels are characterized using the following groupings: LA - Large Arteries (>151 μm), SA- Small Arteries/Arterioles (9-150 μm), Capillaries (<9 μm), SV – Small Venules (9-90 μm), and LV – Large Venules (>90 μm). If multiple pressures for the specific vessel type were reported, an average of the values was used.

Figure 2. (A) Anatomic schematic drawing representing the portion of the rat hindlimb vasculature simulated in this study. Major branches of the rat iliac-femoral system from its origin at the aortic trifurcation to its division into the saphenous and popliteal arteries of the distal limb are shown. The occlusion of the femoral artery is denoted with a large black X. A major collateral artery is labeled (perforating artery in the rat). Pressures labeled in blue (P_a, P_1, P_2, P_{distal}, and P_v) correspond to pressures defined in the theoretical model and depicted in panel B. Thigh and calf regions are labeled, also corresponding to the regions defined in panel B. (B) Vascular network of the rat hindlimb. Blood enters the hindlimb through the common iliac artery (R_{CIA}) which branches into the external iliac artery (R_{EIA}) and internal iliac artery (R_{IIA}). Flow from the internal iliac supplies the thigh region (R_{THIGH}). The EIA leads into the femoral artery (R_{FEM}) which branches into the largest feed arteries (R_{FEED},

diameter >90 μm) in the calf, the most proximal of which is the popliteal artery. The remaining microvasculature of the calf is represented by mid-sized arteries and arterioles (R_{MID}, diameter 9-90 μm) and capillaries (R_{CAP}, diameter < 9 μm. The venous system is lumped into a single compartment (R_{VEIN}). Under non-occluded conditions, a very small amount of flow moves through the collateral pathways from the distal femoral artery to the internal iliac, providing additional blood supply to the thigh [9]. Under conditions of femoral arterial occlusion (occlusion denoted with a red X), flow through the internal iliac supplies both the thigh (directly) and the calf (indirectly through the collateral arteries).

Figure 3. (A) Ratio of occluded to non-occluded calf flow under resting conditions. Acute vascular adaptations are compared. The flow ratio observed in the experimental resting acute case is 0.5 (Table 5) and is depicted as a dashed black line. The four colored curves indicate the theoretical flow restoration with various adaptations simulated: (1) No compensation (blue curve, occluded flow with no changes in vascular adaptations), (2) Dilation of the distal tree (red curve, dilation of mid-sized arteries/arterioles with diameter 9-90 μm), (3) Collateral dilation (green curve, dilation of the collateral arteries by a factor between 1 and 2), and (4) Collateral dilation and dilation of the distal tree (black curve, combined increase in collateral arteries by a factor between 1 and 2 and dilation of mid-sized arteries/arterioles). **(B)** Pressure values (P_a, P_1, P_{distal}, and P_v) throughout theoretical vascular network under resting conditions. The four acute vascular response scenarios from part (A) as well as the non-occluded case (black dashed curve) are depicted.

Figure 4: Ratio of occluded to non-occluded flow given combinations of different vascular adaptations from Table 4. Possible adaptations for acute occlusion are: dilation of distal arterioles (D), 100% dilation of the collateral artery (C), or both (DC). Possible adaptations for chronic occlusion are: structural remodeling of distal arterioles (E), dilation of distal arterioles (D), increased number of capillaries and distal arterioles (G), 100% dilation of the collateral artery (C) or combinations thereof (GC, GCE, GCED). In all chronic vascular adaptation simulations, a 27% enlargement of the collateral arteries is assumed.

Figure 5: Ratio of occluded to non-occluded flow given the presence of all acute responses (green) or all chronic responses (yellow) under both rest and exercise conditions. A 100% increase in collateral diameter is assumed in both cases.

Figure 6: Model-predicted values of collateral dilation factors necessary to obtain experimentally-observed flow (blue) [4] or total compensation (yellow) under rest (A) or exercise (B) conditions given acute or chronic vascular adaptations C (collateral dilation alone) or DC (distal arteriolar dilation and collateral arterial dilation). X's indicate that there is no possible degree of collateral dilation that would yield the desired flow value. Model-predicted values of the ratio of occluded to non-occluded flow are shown as the number of collateral vessels is varied between 0 and 200 for three different sized collateral diameters under rest (C) and exercise (D) conditions. No adaptations to the distal microcirculation are considered in panels (C) or (D).

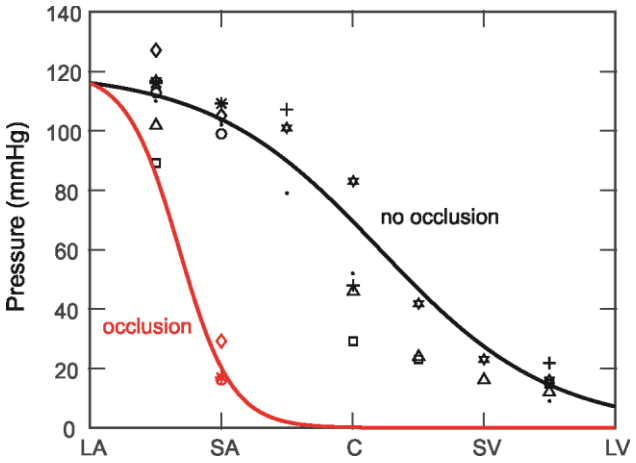

Figure 2